Inorganic Chemistry

Article

pubs.acs.org/IC

Magnetic Relaxations Arising from Spin−Phonon Interactions in the Nonthermally Activated Temperature Range for a Double-Decker Terbium Phthalocyanine Single Molecule Magnet

Takamitsu Fukuda,*[,†] Natsuko Shigeyoshi,[†] Tomoo Yamamura,[‡] and Naoto Ishikawa*[,†]

[†]Department of Chemistry, Graduate School of Science, Osaka University, Toyonaka, Osaka 560-0043, Japan

[‡]Laboratory of Alpha-Ray Emitters, Institute for Materials Research, Tohoku University, Sendai 980-8577, Japan

Supporting Information

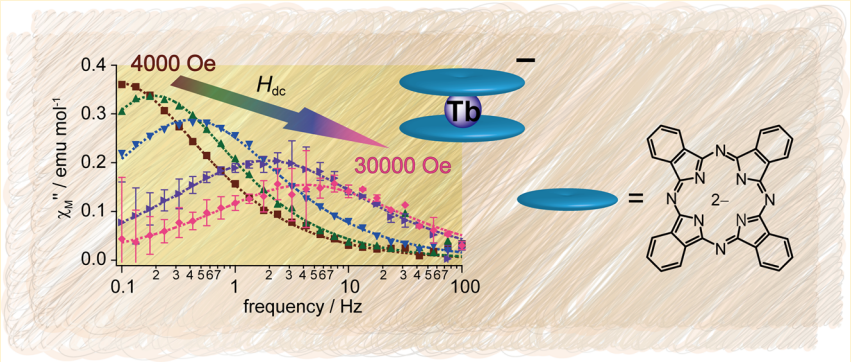

ABSTRACT: Magnetic relaxations arising from spin−phonon interactions for a magnetically diluted double-decker terbium phthalocyanine single molecule magnet, dil**1**, in the nonthermally activated temperature range have been investigated. While the relaxation time, τ, is independent of the external static magnetic field, H_{dc}, in the high temperature range, where linear relationships between $-\ln \tau$ and T^{-1} are observed in the Arrhenius plot, magnetic field dependences for τ are observed in the lower temperature range. The τ^{-1} vs H_{dc} plot at 12 K fits the quadric curve when $H_{dc} < 12$ kOe, while linear relationships are observed in the τ^{-1} vs T plots in the temperature range of 12−20 K. These results indicate that the direct process is the dominant magnetic relaxation pathway in the nonthermally activated temperature range, while the contribution from the Raman process, if any, is not observable. We emphasize in this paper that the contribution from the thermal relaxation processes and the quantum tunneling of magnetizations (QTMs) to the experimentally observed magnetic relaxations must be evaluated carefully in order to avoid confusion between the thermal and quantum-mechanical relaxation pathways.

INTRODUCTION

Magnetic bistabilities realized by single discrete molecules have drawn increasing attention in recent years, since this class of compound is of great significance for development of next-generation information device technology and molecular spintronics.[1] In the early stage of the relevant research field, multinuclear 3d transition metal clusters were examined extensively.[2] Dodecanuclear manganese clusters show slow magnetic relaxations in the temperature range lower than 7 K, where the concept of a single molecule magnet (SMM) has been proposed for the first time.[2b] The mechanism of these unusual magnetic properties realized in SMMs is generally interpreted by assuming a double-well type potential surface which results from the uniaxial magnetic anisotropy and total high spin multiplicities of the assembled metal centers; i.e., the presence of the finite energy barrier impedes free flips between the two degenerate high spin ground states.[3]

On the other hand, a variety of lanthanide complexes have been demonstrated to show slow magnetic relaxation phenomena, since the concept of lanthanide-based single-ion molecule magnets (SIMMs) or, more simply, lanthanide SMMs, first appeared in a paper from our group in 2003.[4,5] The magnetic relaxation mechanism of lanthanide SMMs can be understood in a different way from that of the conventional transition metal cluster SMMs.[6,7] Because of the presence of a strong spin−orbit coupling, the total angular momentum of a free lanthanide ion having an orbital angular momentum of L and a spin angular momentum of S can be described by the LS-couplings, leading to the $(2J + 1)$-fold ground electronic states having the total angular momentum of J, where $J = L + S$ for heavy lanthanide ions. For example, a free terbium ion (Tb^{3+}) has eight 4f electrons and its ground states can be represented by the $^7F_6$ atomic term, meaning that a free Tb^{3+} ion has 13-fold degenerate ground states. Recently, the chemistry of actinide or 3d metal based SIMMs has been developed

Received: May 12, 2014
Published: August 18, 2014

   dx.doi.org/10.1021/ic501028f | *Inorg. Chem.* 2014, 53, 9080−9086

extensively, and these also take advantage of the presence of a large orbital angular momentum at the magnetic center.[8,9]

The presence of crystal or ligand fields around the lanthanide ion, however, lifts the degeneracy of the ground electronic states of the lanthanide ion through the electrostatic or ligand field (LF) potentials. The Hamiltonian corresponding to an LF having a tetragonal symmetry can be written as

$$\mathbf{H}_{\mathrm{LF}} = A_2^0\langle r^2\rangle\alpha\mathbf{O}_2^0 + A_4^0\langle r^4\rangle\beta\mathbf{O}_4^0 + A_4^4\langle r^4\rangle\beta\mathbf{O}_4^4 + A_6^0\langle r^6\rangle\gamma\mathbf{O}_6^0 + A_6^4\langle r^6\rangle\gamma\mathbf{O}_6^4 \quad (1)$$

where the A_k^q coefficients and the $\mathbf{O}_k^q$ operators are adjustable parameters and polynomials of the total angular momentum matrices, $\mathbf{J}^2$, $\mathbf{J}_z$, $\mathbf{J}_-$, and $\mathbf{J}_+$, respectively.[10] The α, β, and γ coefficients are the Stevens parameters.[11]

In general, it is practical to represent the resultant wave functions by using the linear combinations of $|J_z\rangle$ wave functions as the basis sets, where J_z refers to the projection of the J to the quantization axis. In the case where the ligands provide an ideal square-antiprismatic (SAP) LF with the lanthanide ion, however, mixings between the different $|J_z\rangle$ wave functions through the $A_4^4\langle r^4\rangle\beta\mathbf{O}_4^4$ and $A_6^4\langle r^6\rangle\gamma\mathbf{O}_6^4$ terms are symmetry forbidden. Accordingly, the Hamiltonian given in eq 1 can be reduced to

$$\mathbf{H}_{\mathrm{LF}} = A_2^0\langle r^2\rangle\alpha\mathbf{O}_2^0 + A_4^0\langle r^4\rangle\beta\mathbf{O}_4^0 + A_6^0\langle r^6\rangle\gamma\mathbf{O}_6^0 \quad (2)$$

Although there have been limited numbers of this class of highly symmetric lanthanide compounds known so far, some coordination compounds and polyoxometalates (POMs) fulfill these structural requirements.[12] Ishikawa et al. has first demonstrated that the static and dynamic magnetic properties of double-decker type terbium diphthalocyanine complexes ($TbPc_2$, Scheme 1) can be understood based on their electronic

Scheme 1. Structure and Abbreviations of the Anionic Form of Double-Decker Phthalocyanine Complexes

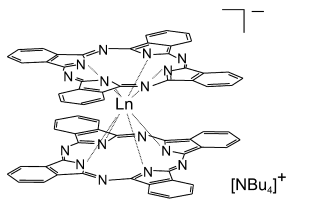

1 : Ln = Tb^{3+}
2 : Ln = Y^{3+}
dil**1** : 2 mol% **1** in **2**

structures, where the ground and second lowest electronic states of the Tb^{3+} ion in the complexes are described by using the almost pure $|\pm6\rangle$ and $|\pm5\rangle$ wave functions, respectively, and the energy difference between these, Δ, reaches several hundred reciprocal centimeters (cm^{-1}).[4,6,7]

In general, the magnetic relaxation rate (τ^{-1}) of a lanthanide complex can be formulated as

$$\tau^{-1} = \frac{1}{\tau_{\mathrm{Orbach}}} + \frac{1}{\tau_{\mathrm{direct}}} + \frac{1}{\tau_{\mathrm{Raman}}} + \frac{1}{\tau_{\mathrm{QTM}}} \quad (3)$$

in which the first three terms in the right-hand side, i.e., the Orbach, direct, and Raman terms, occur due to the energy exchanges between the paramagnetic ions and phonon radiations.[13] On the other hand, the quantum tunneling of magnetization (QTM) term arises from magnetic relaxations caused by transitions between different spin states as a result of the evolution of a two-level system in a time-varying magnetic field without spin−lattice energy exchange.

For terbium-based lanthanide SMMs, the magnetic relaxation phenomena in a high temperature range are dominated by the two-phonon Orbach process; i.e., the ground $|J_z\rangle = |\pm6\rangle$ states are excited to the $|\pm5\rangle$ and/or other states by absorbing a phonon, which is followed by the emission of a second phonon to give the ground states having the sign-reversed J_z. Experimentally, these relaxation pathways can be unambiguously confirmed by observing a linear relationship in the $-\ln\tau$ vs T^{-1} plot, where τ and T are relaxation time and temperature, respectively.[14] In the case of $[TbPc_2]^-TBA^+$ (TBA = tetrabutylammonium), this relationship is observed in the temperature range higher than 25 K in the absence of a static magnetic field.[7] Ruben and co-workers performed a detailed study on spin dynamics of diluted $[TbPc_2]^-TBA^+$ based on solid state ^1H NMR experiments.[15]

In contrast, contribution from the Orbach process becomes negligible when $\Delta \gg kT$, since the excitations from the $|\pm6\rangle$ to $|\pm5\rangle$ states are suppressed in the low temperature range, and instead, nonthermally activated mechanisms such as the direct and Raman processes possibly dominate the magnetic relaxation. Although applications of lanthanide SMMs to high-density memory devices attach great importance to their performance in a high temperature range, quantum-mechanical phenomena for the purpose of the development of a quantum computing system based on $TbPc_2$ have been demonstrated in a rather low temperature range, where nonthermally activated spin−phonon interactions in addition to QTM become more significant.[16] Nevertheless, little attention has been given to the detailed magnetic relaxation dynamics of lanthanide SMMs in the nonthermally activated temperature range, and frequently, the spin−phonon interactions are lumped even together with a QTM regime, although these are fundamentally different phenomena in origin. Recently, we have reported that magnetic relaxations of quadruple-decker diterbium and terbium−yttrium phthalocyanine tetramers are enhanced with increasing the static magnetic field in the low temperature range, and these observations have been ascribed tentatively to the dominant direct process.[17] In the present paper, we report dynamic magnetic properties of a diluted terbium double-decker phthalocyanine SMM, dil**1** (Scheme 1), in the nonthermally activated temperature range in order to deepen our understandings about the magnetic relaxation mechanism of lanthanide SMMs.

EXPERIMENTAL SECTION

Isostructural double-decker phthalocyanine complexes having either a paramagnetic Tb^{3+} ion or a nonmagnetic Y^{3+} ion, **1** and **2** (Scheme 1), were synthesized according to the literature methods with some modifications.[18] Both complexes have closed-shell π-electronic systems. In order to reduce intermolecular magnetic interactions and torquing effects during magnetic measurements to the extent possible, a magnetically diluted solid sample of **1**, namely dil**1**, was prepared and fixed as follows. A mixture of **1** and **2** in a molar ratio of 2:98 was dissolved in hot acetone, and the solution was stirred overnight. Most of the solvent was evaporated in vacuo, and the formed precipitate was collected by vacuum filtration. The residue was passed through a short alumina column chromatograph by using acetone as the eluent. The colored fraction was collected and concentrated in vacuo, from which the microcrystalline sample containing **1** in **2** (2 mol %) was obtained. After the crystals were dried under reduced pressure at 60 °C, the sample (ca. 57 mg) was tightly packed in a straw, and fixed by using

dx.doi.org/10.1021/ic501028f | Inorg. Chem. 2014, 53, 9080−9086

melted eicosane (6 mm in diameter × 9 mm in length). Alternating current (ac) magnetic susceptibility measurements were carried out on Quantum Design MPMS and PPMS magnetometers for the frequency ranges of 0.1−100 and 100−10 000 Hz, respectively. Since magnetic measurements under a high static magnetic field, H_{dc}, reduce signal intensities, the accumulated data obtained at $H_{dc} \geq 20$ kOe were statistically treated.

RESULTS AND DISCUSSION

The temperature dependences of ac susceptibilities for dil**1** at H_{dc}'s of 0 and 8000 Oe indicate that the χ_M'' values are near zero in the temperature range lower than 30 K (Figure 1). At

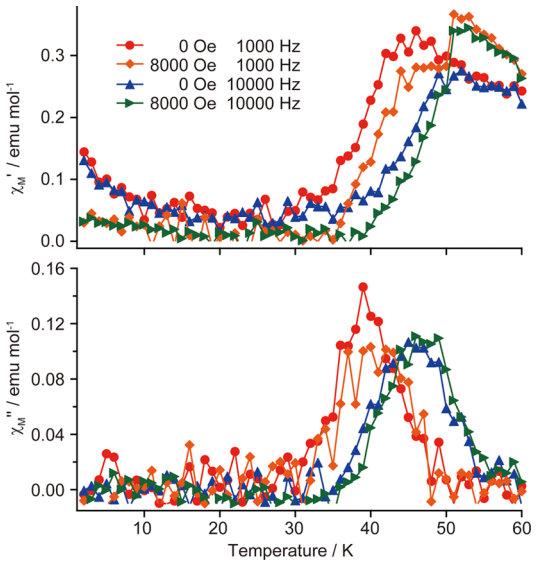

Figure 1. Plots of χ_M' (top) and χ_M'' (bottom) against temperature for dil**1** at external magnetic field (H_{dc}) values of 0 (red circles and blue triangles) and 8000 Oe (orange diamonds and green triangles).

values of the ac magnetic field frequency, f, of 10 000 and 1000 Hz, the peak temperatures appear at ca. 46 and 39 K, respectively, irrespective of H_{dc}. The magnetic relaxations of dil**1** in the high temperature range are dominated by the two-phonon Orbach process, and the observed independences of peak temperatures with respect to H_{dc} are consistent with this assignment; i.e., relaxation processes other than the Orbach process are negligible at the temperature range higher than 30 K.

In order to find appropriate experimental conditions, in which the Orbach process is sufficiently suppressed, and the peak frequency in the χ_M'' vs f plot appears within the experimentally available window ($f \geq 0.1$ Hz), χ_M'' values as a function of f and T were measured at H_{dc} values of 0 and 8000 Oe (Supporting Information, Figures S1 and S2). The natural logarithm of the reciprocal of the relaxation time (τ) at each temperature and H_{dc} extracted by fitting the experimental data on the basis of the Cole−Cole model is plotted against the inverse of the temperature in Figure 2. In the high temperature range ($T > 35$ K), the plots fit straight lines, with the correlation factors (R^2) being higher than 0.99 (red and blue dashed lines). The results of the Cole−Cole fitting at 45 K are shown in Figure 3 as an example. As clearly demonstrated, the frequencies at which the χ_M'' values become the maximum are almost identical at this temperature range irrespective of H_{dc}. The estimated blocking energies, Δ_b's, lie within the range 530−540 cm^{-1}, and the preexponential factors (τ_0^{-1}), almost

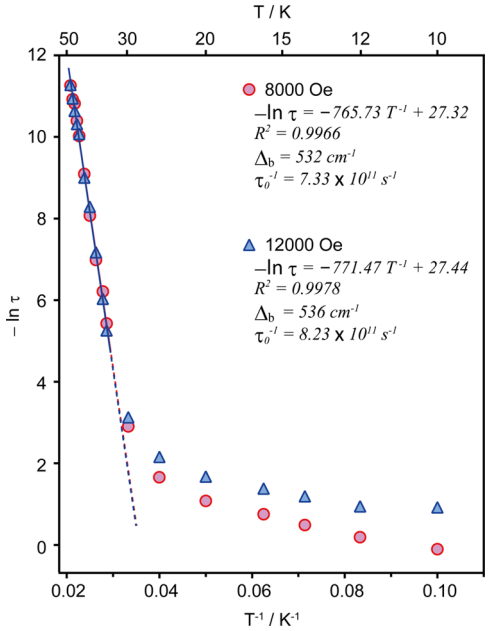

Figure 2. Natural logarithm of the magnetization relaxation time of dil**1** against inverse of the temperature in the presence of external magnetic field (H_{dc}) values of 8000 (red circles) and 12 000 Oe (blue triangles). The regression lines obtained in the temperature range 48−35 K for each H_{dc} also are shown as dashed straight lines. The corresponding regression formulas, correlation factors (R^2), blocking energies, and preexponential factors are given in the upper right.

reach the order of 10^{12} s^{-1}. These observations indicate that the Orbach process is dominant as the magnetic relaxation mechanism in this temperature range, since the Orbach process is independent of an external magnetic field unless it alters the value of Δ_b.[10] On the other hand, the plots deviate from the regression lines at temperatures lower than 30 K (Figure 2). It should be noted that the $-\ln \tau$ values are dependent on the temperature even in the low temperature range. In addition, the relaxation times depend also on H_{dc} in this temperature range. Since H_{dc} of 8000 Oe is sufficiently large to suppress the QTM for **1**,[19] the observed field dependences indicate that the spin−phonon mechanism is largely involved with the magnetic relaxation phenomena. That is, the magnetic relaxation rate given in eq 3 can be simplified to eq 4 on the condition of low temperature and $H_{dc} \gg 0$.

$$\tau^{-1} = \frac{1}{\tau_{direct}} + \frac{1}{\tau_{Raman}} \quad (4)$$

The lowest temperature at which the peak frequencies can be accurately determined in the χ_M'' vs f plot is 12 K as seen in Figure 2 and the Supporting Information, Figures S1 and S2.

The magnetization vs magnetic field (**M**−**H**) plot of dil**1** measured at 12 K is given in Figure 4. The magnetization is proportional to **H** in the region of ca. |**H**| < 1.5 T, and the slope decreases gradually beyond this region, leading finally to plateaus at ca. **H** = ±5 T. The curvature in Figure 4 indicates that the relative detection sensitivity for ac magnetic susceptibility values lowers significantly at the H_{dc} value higher than approximately 3−4 T.

Figure 5a depicts the plots of χ_M' and χ_M'' against f for dil**1** at 12 K, and Figure 5b depicts the corresponding Cole−Cole plots, demonstrating the field dependences of τ at the fixed temperature. Based on the fitting curves, the peak appears at 0.5

dx.doi.org/10.1021/ic501028f | Inorg. Chem. 2014, 53, 9080−9086

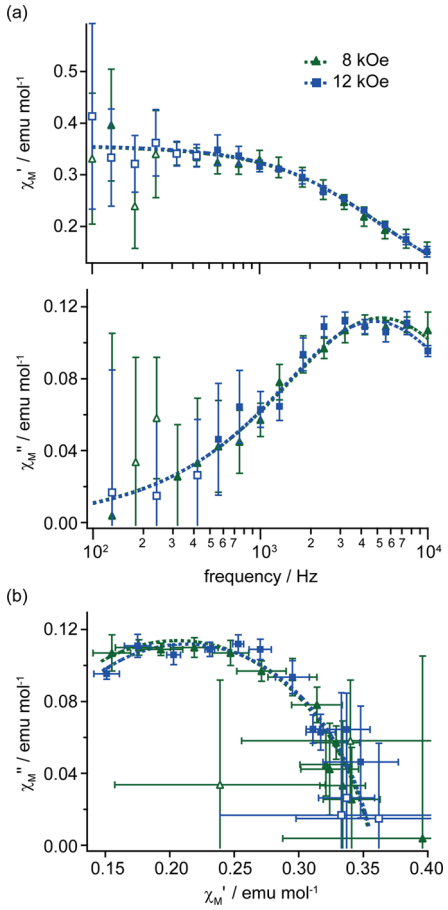

Figure 3. (a) Plots of χ_M' (top) and χ_M'' (bottom) against applied ac frequency f for dil**1** and (b) Cole−Cole plots for dil**1** at external magnetic fields of 8000 (green triangles) and 12 000 Oe (blue squares) at 45 K. Error bars represent standard deviations. Open symbols are omitted for the fitting procedure. See the Supporting Information for the data obtained at other temperatures.

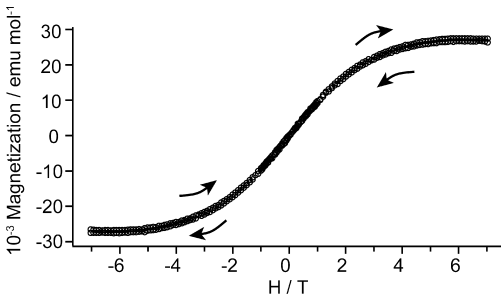

Figure 4. Magnetization vs field plot of dil**1** measured at 12 K.

Hz in the χ_M'' vs f plot at H_{dc} = 0 Oe (gray circles), which shifts to 0.09 Hz at H_{dc} = 4000 Oe (brown squares); i.e., the magnetic relaxations are efficiently suppressed by applying the static magnetic field. In the region where H_{dc} is less than ca. 500 Oe, the theoretically calculated Zeeman diagram of **1** (see Figure 3 in ref 19) indicates that admixture of the $|+6\rangle$ and $|-6\rangle$ wave functions through the hyperfine interactions between J and the nuclear spin of the terbium ion possibly promotes the QTMs, resulting in shorter τ.[19] In contrast, the H_{dc} value of 4000 Oe or higher corresponds to the region distinctly outside the crossing area in the Zeeman diagram, and therefore, suppression of the QTM is anticipated at H_{dc} > 4000 Oe. With

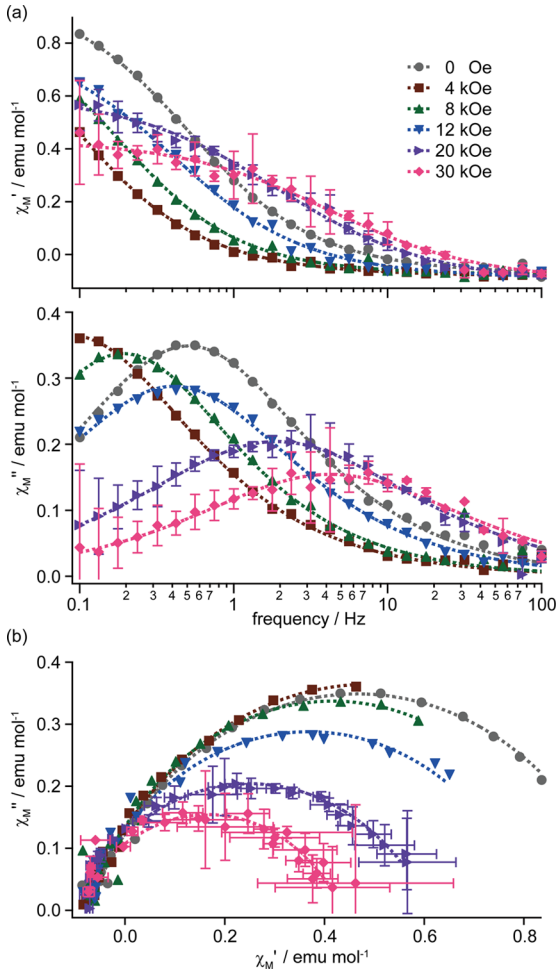

Figure 5. (a) Plots of χ_M' (top) and χ_M'' (bottom) against applied ac frequency f for dil**1** at various values of the external magnetic field (H_{dc}, ranging from 0 to 30 000 Oe) at 12 K. (b) Cole−Cole plots for dil**1** at various H_{dc}'s. Error bars shown for H_{dc} values of 20 and 30 kOe represent standard deviations.

increasing H_{dc} at 12 K, the peak shifts to the higher frequency side in the χ_M'' vs f plot (Figure 5a, bottom). In other words, the magnetic relaxations are promoted by the presence of the static magnetic field, even though neither the Orbach nor the QTM process is dominant under the employed conditions. The Cole−Cole plots can be simulated by assuming the single relaxation component with the dispersion coefficients, α, being less than 0.35 (see Table S1 in the Supporting Information for full fitting parameters). We have also confirmed that similar relationships are observed even at 20 K, indicating that the contribution from the Orbach process is practically negligible at temperatures lower than 20 K (Supporting Information, Figure S3).

Spin−phonon relaxation rates in the nonthermally activated temperature range are interpreted by the direct and Raman processes. By taking the first order Zeeman interaction into consideration, the former process occurring between the initially degenerate $|+6\rangle$ and $|-6\rangle$ states of a non-Kramers terbium ion can be formulated as

$$\tau_{direct}^{-1} \propto H_{dc}^{3} \coth(6g_J\mu_B H_{dc}/kT) \quad (5)$$

or

dx.doi.org/10.1021/ic501028f | Inorg. Chem. 2014, 53, 9080−9086

$$\tau_{direct}^{-1} \propto H_{dc}^{2}T \qquad \text{when } 6g_J\beta H_{dc}/kT \ll 1 \tag{6}$$

where g_J, μ_B, and k are the Landé g-factor, Bohr magneton, and Boltzmann constant, respectively, while the latter predicts a $\tau_{Raman}^{-1} \propto T^7$ relationship.[10,20]

Figure 6 shows the plots of τ^{-1} values estimated from the Cole−Cole plots against H_{dc} at 12 K. The experimental results

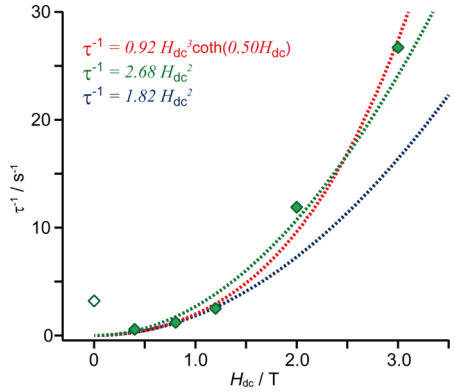

Figure 6. Plots of inverse of magnetization relaxation time (τ) against H_{dc} at 12 K (green diamonds). The regression curves are shown as dotted lines with the corresponding regression formulas given in the upper left. Note that the open symbol at H_{dc} = 0 T was omitted for the regression analyses, since contributions from the QTM relaxation pathway to τ can be neglected only when $H_{dc} \gg 0$. The blue curve fits the points at the lower H_{dc} only, while all data were considered to obtain the green and red fitting curves.

(filled green diamonds) satisfactorily fit the quadric equation in the low H_{dc} region (blue dotted line), indicating that τ^{-1} varies as the square of the external static magnetic field. At higher H_{dc}, the best fit was obtained by using a hyperbolic cotangent function (red dotted line) rather than the approximate quadric curve (green dotted line). These observations strongly suggest that the direct process is one of the pivotal magnetic relaxation pathways at 12 K, and eq 6 can be employed to fit the experimental results in terms of H_{dc} less than 12 kOe. At H_{dc} = 0 Oe, the τ^{-1} value (open diamond) deviates from the fitting curves due to the nonnegligible contribution from the QTMs. See Figure S4 in the Supporting Information for the corresponding plots prepared based on the data obtained at 20 K.

In order to confirm the validity of eq 6 and, further, to estimate the contribution from the Raman process, the relationships between τ^{-1} and temperature are plotted in Figure 7. As clearly demonstrated, the τ^{-1} values vary linearly as the temperature between 12 and 20 K with the correlation factors being higher than 0.99. Therefore, it can be concluded that the Raman process is not observable within the limit of experimental accuracy, and the direct process dominates as the magnetic relaxation pathway in this temperature range. The plots deviate from the regression lines irrespective of H_{dc} at 25 K due presumably to the concurrent occurrence of the Orbach and direct processes, being consistent with the results shown in Figure 2. On the other hand, the mismatches observed at 10 K can be ascribed neither to the Orbach process nor to QTM phenomena. In the low temperature limit, the hyperbolic cotangent term in eq 5 approaches 1, and as a result, τ^{-1} also converges to a constant value. This relationship is demonstrated in Figure S5 in the Supporting Information; i.e., the linearity of eq 5 is valid only in the high temperature range, and

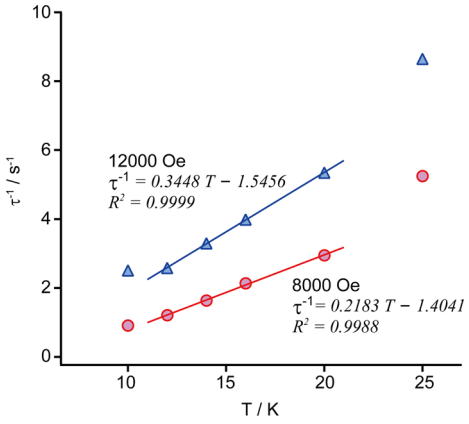

Figure 7. Plots of inverse of magnetization relaxation time against temperature in the presence of H_{dc} values of 8000 (red circles) and 12 000 Oe (blue triangles). The regression lines obtained in the temperature range of 12−20 K for each H_{dc} also are shown accompanied by the corresponding regression formulas and correlation factors.

the slope decreases with decreasing temperature, leading finally to constant τ^{-1} values. Under our experimental conditions employed in Figure 7, i.e., at H_{dc} = 12 kOe and the temperature range between 12 and 20 K, the linearity of eq 5 is maintained. Although the deviations of the plots from the regression lines at 10 K are presumably interpreted on the basis of eq 5, we do not exclude the possibility that the deviations arise from the experimental errors in the present study.

CONCLUSIONS

In the present paper, we have demonstrated that magnetic relaxation time, τ, observed in the nonthermally activated temperature range of a magnetically diluted double-decker terbium phthalocyanine single molecule magnet, dil**1**, is largely dependent on the external static magnetic field, H_{dc}, and temperature under the conditions where the QTM phenomena are sufficiently suppressed. The τ^{-1} vs H_{dc} plot at 12 K fits the quadric curve, while the linear relationship is observed in the τ^{-1} vs T plot in the temperature range 12−20 K. These observations strongly indicate that the magnetic relaxations are dominated by the direct process as a result of thermal spin−phonon interactions between the magnetic center (Tb^{3+}) and the crystal lattice rather than the Raman process. Although the physics of magnetic dynamics of inorganic salts containing lanthanide ions had already been established in the 1960s,[10] to the best of our knowledge, few reports discuss the nonthermally activated relaxation processes for lanthanide SMMs in detail. As a consequence, the thermal processes and QTMs are mixed up as a "QTM regime" in certain cases, although these processes are fundamentally different from each other in origin. Recent seminal works on $TbPc_2$-based spintronic devices have reported that molecular spin valve or spin resonator functions have been realized by cooperative direct and QTM relaxation mechanisms at low temperatures (<1 K).[21] The present paper suggests that contributions from the thermal relaxation processes and the QTMs to the experimentally observed magnetic relaxation phenomena must be evaluated carefully in order to deepen our understandings of the spin dynamics for lanthanide SMMs especially in the low temperature range.

dx.doi.org/10.1021/ic501028f | Inorg. Chem. 2014, 53, 9080−9086

■ ASSOCIATED CONTENT

Supporting Information

Results of Cole−Cole fittings. Effect of external magnetic field on magnetic relaxation rates at 20 K. Comparison of linear and hyperbolic cotangent functions. Fitting parameters. This material is available free of charge via the Internet at http://pubs.acs.org.

■ AUTHOR INFORMATION

Corresponding Authors

*E-mail: tfukuda@chem.sci.osaka-u.ac.jp.
*E-mail: iskw@chem.sci.osaka-u.ac.jp.

Author Contributions

The manuscript was written through contributions of all authors. All authors have given approval to the final version of the manuscript.

Notes

The authors declare no competing financial interest.

■ ACKNOWLEDGMENTS

This work was performed under the Interuniversity Cooperative Research Program of the Institute for Materials Research, Tohoku University (Proposal No. 13K0068 and No. 14K0060).

■ REFERENCES

(1) (a) Ladd, T. D.; Jelezko, F.; Laflamme, R.; Nakamura, Y.; Monroe, C.; O'Brien, J. L. *Nature* **2010**, *464*, 45. (b) Bogani, L.; Wernsdorfer, W. *Nat. Mater.* **2008**, *7*, 179. (c) Thomas, L.; Lionti, F.; Ballou, R.; Gatteschi, D.; Sessoli, R.; Barbara, B. *Nature* **1996**, *383*, 145. (d) Friedman, J. R.; Sarachik, M. P.; Tejada, J.; Ziolo, R. *Phys. Rev. Lett.* **1996**, *76*, 3830.

(2) (a) Sessoli, R.; Tsai, H. L.; Schake, A. R.; Wang, S. Y.; Vincent, J. B.; Folting, K.; Gatteschi, D.; Christou, G.; Hendrickson, D. N. *J. Am. Chem. Soc.* **1993**, *115*, 1804. (b) Sessoli, R.; Gatteschi, D.; Caneschi, A.; Novak, M. A. *Nature* **1993**, *365*, 141. (c) Eppley, H. J.; Tsai, H. L.; de Vries, N.; Folting, K.; Christou, G.; Hendrickson, D. N. *J. Am. Chem. Soc.* **1995**, *117*, 301. (d) Aubin, S. M. J.; Sun, Z. M.; Pardi, L.; Krzystek, J.; Folting, K.; Brunel, L. C.; Rheingold, A. L.; Christou, G.; Hendrickson, D. N. *Inorg. Chem.* **1999**, *38*, 5329. (e) Soler, M.; Chandra, S. K.; Ruiz, D.; Davidson, E. R.; Hendrickson, D. N.; Christou, G. *Chem. Commun.* **2000**, 2417. (f) Boskovic, C.; Pink, M.; Huffman, J. C.; Hendrickson, D. N.; Christou, G. *J. Am. Chem. Soc.* **2001**, *123*, 9914. (g) Aubin, S. M. J.; Dilley, N. R.; Pardi, L.; Krzystek, J.; Wemple, M. W.; Brunel, L. C.; Maple, M. B.; Christou, G.; Hendrickson, D. N. *J. Am. Chem. Soc.* **1998**, *120*, 4991. (h) Aubin, S. M. J.; Wemple, M. W.; Adams, D. M.; Tsai, H. L.; Christou, G.; Hendrickson, D. N. *J. Am. Chem. Soc.* **1996**, *118*, 7746. (i) Andres, H.; Basler, R.; Güdel, H. U.; Aromi, G.; Christou, G.; Büttner, H.; Rufflé, B. *J. Am. Chem. Soc.* **2000**, *122*, 12469. (j) Sangregorio, C.; Ohm, T.; Paulsen, C.; Sessoli, R.; Gatteschi, D. *Phys. Rev. Lett.* **1997**, *78*, 4645. (k) Aubin, S. M. J.; Spagna, S.; Eppley, H. J.; Sager, R. E.; Christou, G.; Hendrickson, D. N. *Chem. Commun.* **1998**, 803.

(3) Gatteschi, D.; Sessoli, R. *Angew. Chem., Int. Ed.* **2003**, *42*, 268.

(4) Ishikawa, N.; Sugita, M.; Ishikawa, T.; Koshihara, S.; Kaizu, Y. *J. Am. Chem. Soc.* **2003**, *125*, 8694.

(5) (a) Car, P. E.; Perfetti, M.; Mannini, M.; Favre, A.; Caneschi, A.; Sessoli, R. *Chem. Commun.* **2011**, *47*, 3751. (b) Cucinotta, G.; Perfetti, M.; Luzon, J.; Etienne, M.; Car, P. E.; Caneschi, A.; Calvez, G.; Bernot, K.; Sessoli, R. *Angew. Chem., Int. Ed.* **2012**, *51*, 1606. (c) Boulon, M. E.; Cucinotta, G.; Luzon, J.; Degl'Innocenti, C.; Perfetti, M.; Bernot, K.; Calvez, G.; Caneschi, A.; Sessoli, R. *Angew. Chem., Int. Ed.* **2013**, *52*, 350. (d) Watanabe, A.; Yamashita, A.; Nakano, M.; Yamamura, T.; Kajiwara, T. *Chem.—Eur. J.* **2011**, *17*, 7428. (e) Jiang, S.; Wang, B.; Sun, H.; Wang, Z.; Gao, S. *J. Am. Chem. Soc.* **2011**, *133*, 4730. (f) Jiang, S.; Liu, S.; Zhou, L.; Wang, B.; Wang, Z.; Gao, S. *Inorg. Chem.* **2012**, *51*, 3079. (g) Jeletic, M.; Lin, P.; Le Roy, J. J.; Korobkov, I.; Gorelsky, S. I.; Murugesu, M. *J. Am. Chem. Soc.* **2011**, *133*, 19286. (h) Liu, J. L.; Yuan, K.; Leng, J. D.; Ungur, L.; Wernsdorfer, W.; Guo, F. S.; Chibotaru, L. F.; Tong, M. L. *Inorg. Chem.* **2012**, *51*, 8538. (i) Williams, U. J.; Mahoney, B. D.; DeGregorio, P. T.; Carroll, P. J.; Nakamaru-Ogiso, E.; Kikkawac, J. M.; Schelter, E. J. *Chem. Commun.* **2012**, *48*, 5593. (j) Thielemann, D. T.; Klinger, M.; Wolf, T. J. A.; Lan, Y.; Wernsdorfer, W.; Busse, M.; Roesky, P. W.; Unterreiner, A. N.; Powell, A. K.; Junk, P. C.; Deacon, G. B. *Inorg. Chem.* **2011**, *50*, 11990. (k) Bhunia, A.; Gamer, M. T.; Ungur, L.; Chibotaru, L. F.; Powell, A. K.; Lan, Y.; Roesky, P. W.; Menges, F.; Riehn, C.; Niedner-Schattenberg, G. *Inorg. Chem.* **2012**, *51*, 9589. (l) Jiang, S.; Wang, B.; Su, G.; Wang, Z.; Gao, S. *Angew. Chem., Int. Ed.* **2010**, *49*, 7448. (m) Bi, Y.; Guo, Y.; Zhao, L.; Guo, Y.; Lin, S.; Jiang, S.; Tang, J.; Wang, B.; Gao, S. *Chem.—Eur. J.* **2011**, *17*, 12476. (n) Wang, Y.; Li, X.; Wang, T.; Song, Y.; You, X. *Inorg. Chem.* **2010**, *49*, 969. (o) Li, D.; Wang, T.; Li, C.; Liu, D.; Li, Y.; You, X. *Chem. Commun.* **2010**, *46*, 2929. (p) Li, X. L.; Chen, C. L.; Gao, Y. L.; Liu, C. M.; Feng, X. L.; Gui, Y. H.; Fang, S. M. *Chem.—Eur. J.* **2012**, *18*, 14632. (q) Li, D.; Zhang, X.; Wang, T.; Ma, B.; Li, C.; Li, Y.; You, X. *Chem. Commun.* **2011**, *47*, 6867. (r) Pointillart, F.; Klementieva, S.; Kuropatov, V.; Le Gal, Y.; Golhen, S.; Cador, O.; Cherkasov, V.; Ouahab, L. *Chem. Commun.* **2012**, *48*, 714. (s) Menelaou, M.; Ouharrou, F.; Rodríguez, L.; Roubeau, O.; Teat, S. J.; Aliaga-Alcalde, N. *Chem.—Eur. J.* **2012**, *18*, 11545.

(6) Ishikawa, N.; Sugita, M.; Okubo, T.; Tanaka, N.; Iino, T.; Kaizu, Y. *Inorg. Chem.* **2003**, *42*, 2440.

(7) Ishikawa, N.; Sugita, M.; Ishikawa, T.; Koshihara, S.; Kaizu, Y. *J. Phys. Chem. B* **2004**, *108*, 11265.

(8) (a) Rinehart, J. D.; Meihaus, K. R.; Long, J. R. *J. Am. Chem. Soc.* **2010**, *132*, 7572. (b) Rinehart, J. D.; Long, J. R. *J. Am. Chem. Soc.* **2009**, *131*, 12558. (c) Mills, D. P.; Moro, F.; McMaster, J.; van Slageren, J.; Lewis, W.; Blake, A. J.; Liddle, S. T. *Nat. Chem.* **2011**, *3*, 454. (d) Magnani, N.; Apostolidis, C.; Morgenstern, A.; Colineau, E.; Griveau, J. C.; Bolvin, H.; Walter, O.; Caciuffo, R. *Angew. Chem., Int. Ed.* **2011**, *50*, 1696. (e) Moro, F.; Mills, D. P.; Liddle, S. T.; van Slageren, J. *Angew. Chem., Int. Ed.* **2013**, *52*, 3430. (f) Antunes, M. A.; Pereira, L. C. J.; Santos, I. C.; Mazzanti, M.; Marcalo, J.; Almeida, M. *Inorg. Chem.* **2011**, *50*, 9915. (g) Meihaus, K.; Rinehart, J. D.; Long, J. R. *Inorg. Chem.* **2011**, *50*, 8484.

(9) (a) Freedman, D. E.; Harman, W. H.; Harris, T. D.; Long, G. J.; Chang, C. J.; Long, J. R. *J. Am. Chem. Soc.* **2010**, *132*, 1224. (b) Gomez-Coca, S.; Cremades, E.; Aliaga-Alcalde, N.; Ruiz, E. *J. Am. Chem. Soc.* **2013**, *135*, 7010. (c) Fortier, S.; Le Roy, J. J.; Chen, C.-H.; Vieru, V.; Murugesu, M.; Chibotaru, L. F.; Mindiola, D. J.; Caulton, K. G. *J. Am. Chem. Soc.* **2013**, *135*, 14670. (d) Maganas, D.; Sottini, S.; Kyritsis, P.; Groenen, E. J. J.; Neese, F. *Inorg. Chem.* **2011**, *50*, 8741. (e) Zadrozny, J. M.; Liu, J.; Piro, N. A.; Chang, C. J.; Hill, S.; Long, J. R. *Chem. Commun.* **2012**, *48*, 3897. (f) Palii, A. V.; Clemente-Juan, J. M.; Coronado, E.; Klokishner, S. I.; Ostrovsky, S. M.; Reu, O. S. *Inorg. Chem.* **2010**, *49*, 8073. (g) Karasawa, S.; Koga, N. *Inorg. Chem.* **2011**, *50*, 5186. (h) Zadrozny, J. M.; Long, J. R. *J. Am. Chem. Soc.* **2011**, *133*, 20732. (i) Jurca, T.; Farghal, A.; Lin, P.-H.; Korobkov, I.; Murugesu, M.; Richeson, D. S. *J. Am. Chem. Soc.* **2011**, *133*, 15814.

(10) Abragam, A.; Bleaney, B. *Electron Paramagnetic Resonance*; Clarendon Press: Oxford, U.K., 1970.

(11) Stevens, K. W. H. *Proc. Phys. Soc. A* **1962**, *65*, 209.

(12) (a) Woodruff, D. N.; Winpenny, R. E. P.; Layfield, R. A. *Chem. Rev.* **2013**, *113*, 5110. (b) Sorace, L.; Benelli, C.; Gatteschi, D. *Chem. Soc. Rev.* **2011**, *40*, 3092. (c) Ishikawa, N. *Polyhedron* **2007**, *26*, 2147. (d) AlDamen, M. A.; Clemente-Juan, J. M.; Coronado, E.; Marti-Gastaldo, C.; Gaita-Arino, A. *J. Am. Chem. Soc.* **2008**, *130*, 8874. (e) AlDamen, M. A.; Cardona-Serra, S.; Clemente-Juan, J. M.; Coronado, E.; Gaita-Ariño, A.; Martí-Gastaldo, C.; Luis, F.; Montero, O. *Inorg. Chem.* **2009**, *48*, 3467. (f) Luis, F.; Martínez-Perez, M. J.; Montero, O.; Coronado, E.; Cardona-Serra, S.; Martí-Gastaldo, C.; Clemente-Juan, J. M.; Sesé, J.; Drung, D.; Schurig, T. *Phys. Rev. B* **2010**, *82*, 060403. (g) Ritchie, C.; Speldrich, M.; Gable, R. W.; Sorace, L.; Kögerler, P.; Boskovic, C. *Inorg. Chem.* **2011**, *50*, 7004.

(13) One of the reviewers indicates the importance of including the multilevel character of the relaxation phenomena in eq 3, which however, is not taken into account in the present study for simplicity.
(14) (a) Coronado, E.; Gimenez-Saiz, C.; Recuenco, A.; Tarazon, A.; Romero, F. M.; Camon, A.; Luis, F. *Inorg. Chem.* **2011**, *50*, 7370. (b) Pointillart, F.; Bernot, K.; Poneti, G.; Sessoli, R. *Inorg. Chem.* **2012**, *51*, 12218. (c) Tian, H.; Liu, R.; Wang, X.; Yang, P.; Li, Z.; Li, L.; Liao, D. *Eur. J. Inorg. Chem.* **2009**, 4498. (d) Xu, J. X.; Ma, Y.; Liao, D. Z.; Xu, G. F.; Tang, J.; Wang, C.; Zhou, N.; Yan, S. P.; Cheng, P.; Li, L. C. *Inorg. Chem.* **2009**, *48*, 8890. (e) Wang, X.; Li, L.; Liao, D. *Inorg. Chem.* **2010**, *49*, 4735.
(15) Branzoli, F.; Carretta, P.; Filibian, M.; Zoppellaro, G.; Graf, M. J.; Galan-Mascaros, J. R.; Fuhr, O.; Brink, S.; Ruben, M. *J. Am. Chem. Soc.* **2009**, *131*, 4387.
(16) Vincent, R.; Klyatskaya, S.; Ruben, M.; Wernsdorfer, W.; Balestro, F. *Nature* **2012**, *488*, 357.
(17) Fukuda, T.; Matsumura, K.; Ishikawa, N. *J. Phys. Chem. A* **2013**, *117*, 10447.
(18) (a) De Cian, A.; Moussavi, M.; Fischer, J.; Weiss, R. *Inorg. Chem.* **1985**, *24*, 3162. (b) Konami, H.; Hatano, M.; Tajiri, A. *Chem. Phys. Lett.* **1989**, *160*, 163.
(19) Ishikawa, N.; Sugita, M.; Wernsdorfer, W. *Angew. Chem., Int. Ed.* **2005**, *44*, 2931.
(20) Scott, P. L.; Jeffries, C. D. *Phys. Rev.* **1962**, *127*, 32.
(21) (a) Urdampilleta, M.; Klyatskaya, S.; Cleuziou, J.-P.; Ruben, M.; Wernsdorfer, W. *Nat. Mater.* **2011**, *10*, 502. (b) Ganzhorn, M.; Klyatskaya, S.; Ruben, M.; Wernsdorfer, W. *Nat. Nanotechnol.* **2013**, *8*, 165.